

Harnessing quantum transport by transient chaos

Rui Yang, Liang Huang, Ying-Cheng Lai, Celso Grebogi, and Louis M. Pecora

Citation: *Chaos* **23**, 013125 (2013); doi: 10.1063/1.4790863

View online: <http://dx.doi.org/10.1063/1.4790863>

View Table of Contents: <http://chaos.aip.org/resource/1/CHAOEH/v23/i1>

Published by the [American Institute of Physics](#).

Related Articles

Lifetime statistics of quantum chaos studied by a multiscale analysis
Appl. Phys. Lett. **100**, 184101 (2012)

Finite-time stochastic combination synchronization of three different chaotic systems and its application in secure communication
Chaos **22**, 023109 (2012)

Characteristics of level-spacing statistics in chaotic graphene billiards
Chaos **21**, 013102 (2011)

Chaotic dephasing in a double-slit scattering experiment
Chaos **20**, 043118 (2010)

The influence of dissipation on the quantum-classical correspondence: Stability of stochastic trajectories
J. Chem. Phys. **130**, 234107 (2009)

Additional information on Chaos

Journal Homepage: <http://chaos.aip.org/>

Journal Information: http://chaos.aip.org/about/about_the_journal

Top downloads: http://chaos.aip.org/features/most_downloaded

Information for Authors: <http://chaos.aip.org/authors>

ADVERTISEMENT



AIP Advances

Submit Now

**Explore AIP's new
open-access journal**

- **Article-level metrics
now available**
- **Join the conversation!
Rate & comment on articles**

Harnessing quantum transport by transient chaos

Rui Yang,¹ Liang Huang,^{1,2} Ying-Cheng Lai,^{1,3,4} Celso Grebogi,⁴ and Louis M. Pecora⁵

¹*School of Electrical, Computer, and Energy Engineering, Arizona State University, Tempe, Arizona 85287, USA*

²*Institute of Computational Physics and Complex Systems, and Key Laboratory for Magnetism and Magnetic Materials of MOE, Lanzhou University, Lanzhou, Gansu 730000, China*

³*Department of Physics, Arizona State University, Tempe, Arizona 85287, USA*

⁴*Institute for Complex Systems and Mathematical Biology, School of Natural and Computing Sciences, King's College, University of Aberdeen, Aberdeen AB24 3UE, United Kingdom*

⁵*Materials Physics and Sensors, US Naval Research Laboratory, Washington, DC 20375, USA*

(Received 9 October 2012; accepted 23 January 2013; published online 21 February 2013)

Chaos has long been recognized to be generally advantageous from the perspective of control. In particular, the infinite number of unstable periodic orbits embedded in a chaotic set and the intrinsically sensitive dependence on initial conditions imply that a chaotic system can be controlled to a desirable state by using small perturbations. Investigation of chaos control, however, was largely limited to nonlinear dynamical systems in the classical realm. In this paper, we show that chaos may be used to modulate or harness quantum mechanical systems. To be concrete, we focus on quantum transport through nanostructures, a problem of considerable interest in nanoscience, where a key feature is conductance fluctuations. We articulate and demonstrate that chaos, more specifically transient chaos, can be effective in modulating the conductance-fluctuation patterns. Experimentally, this can be achieved by applying an external gate voltage in a device of suitable geometry to generate classically inaccessible potential barriers. Adjusting the gate voltage allows the characteristics of the dynamical invariant set responsible for transient chaos to be varied in a desirable manner which, in turn, can induce continuous changes in the statistical characteristics of the quantum conductance-fluctuation pattern. To understand the physical mechanism of our scheme, we develop a theory based on analyzing the spectrum of the generalized non-Hermitian Hamiltonian that includes the effect of leads, or electronic waveguides, as self-energy terms. As the escape rate of the underlying non-attracting chaotic set is increased, the imaginary part of the complex eigenenergy becomes increasingly large so that pointer states are more difficult to form, making smoother the conductance-fluctuation pattern. © 2013 American Institute of Physics. [<http://dx.doi.org/10.1063/1.4790863>]

Controlling quantum-mechanical systems is generally a challenging problem in science and engineering. In this paper, we exploit the idea that chaos may be used to harness certain statistical features of quantum transport dynamics. While previous works elucidated the basic physics underlying the effect of chaos on quantum transport, we propose a scheme that can be implemented experimentally to systematically harness conductance fluctuations associated with quantum transport through nanostructures. Our idea can be illustrated by using a Sinai-type of open billiard quantum dot (QD), where a central circular region forbidden to classical trajectories can be generated by applying a relatively high gate voltage, and the size of the region can be controlled in a continuous manner. Since the system is open, chaos in the classical limit must be transient. We demonstrate for both non-relativistic (semiconductor two-dimensional electron gas (2DEG)) and relativistic (graphene) quantum-dot systems that, when the radius of the central potential region is varied so that the characteristics of the corresponding classical chaotic dynamics are modified, the quantum conductance-fluctuation patterns can be effectively modulated. While a semiclassical argument based on previous works on quantum chaotic scattering can be used to explain qualitatively the role of classical

transient chaos of different dynamical characteristics in affecting the conductance fluctuations, we develop a formal theory based on the concept of self-energies and the complex eigenvalue spectrum of the corresponding generalized non-Hermitian Hamiltonian. The emergence of narrow resonances can be related to the magnitude of the imaginary part of the eigenvalues, and we obtain an explicit formula predicting the form of the narrow resonance. Our theory indicates that the role of continuously varying chaos in the classical limit lies in removing successively the eigenvalues with extremely small imaginary parts. Our results suggest a viable way to harness quantum behaviors of nanostructures, which can be of interest due to the feasibility of experimental implementation of our scheme.

I. INTRODUCTION

Controlling chaos in dynamical systems has been studied for more than two decades since the seminal work of Ott, Grebogi, and Yorke.¹ The basic idea was that chaos, while signifying random or irregular behavior, should not be viewed as a nuisance in applications of nonlinear dynamical

systems. In fact, given a chaotic system, that there is an infinite number of unstable periodic orbits embedded in the underlying chaotic invariant set means that there are an equally infinite number of choices for the operational state of the system depending on need, provided that any such state can be stabilized. Then, the intrinsically sensitive dependence on initial conditions, the hallmark of any chaotic system, implies that it is possible to apply small perturbations to stabilize the system about any desirable state. Controlling chaos has since been studied extensively and examples of successful experimental implementation abound in physical, chemical, biological, and engineering systems.² The vast literature on controlling chaos, however, has been limited to nonlinear dynamical systems in the classical domain. The purpose of this paper is to elaborate the recent idea that chaos may be exploited to harness or modulate quantum-mechanical behaviors^{3,4} by presenting a systematic study of the role of transient chaos in modulating quantum transport dynamics.

A fundamental quantity characterizing the transport of an electron through a nanostructure, such as a quantum dot or a quantum point contact, is quantum transmission probability, or simply quantum transmission. In general, quantum transmission is determined by many electronic and system parameters such as the Fermi energy, the strength of external magnetic field (if there is one), and the details of the geometry of the structure. If the structure is connected through electronic waveguides (or leads) to electron reservoirs (i.e., contacts) to form a circuit, the conductances defined with respect to various voltage biases among the contacts, together with the corresponding currents, will be determined by the quantum transmission.⁵ This means that the conductances can also depend sensitively on electronic and geometrical parameters. For example, as the Fermi energy of the electronic system changes, the conductances can exhibit wild and sharp fluctuations.⁶ In applications such as the development of electronic circuits and nanoscale sensors, severe conductance fluctuations are undesirable and are to be eliminated so that stable device operation can be achieved. The outstanding question is then, can practical and experimentally feasible schemes be articulated to modulate the quantum conductance fluctuations? We shall demonstrate and provide theoretical understanding that classical *transient chaos* can be used to effectively modulate conductance-fluctuation patterns associated with quantum transport through nanostructures.

Intuitively, the basic principle underlying our transient-chaos based strategy for modulating quantum transport can be explained, as follows. It is known that quantum pointer states, which are resonant states of finite but long lifetime formed inside the nanostructure,⁷ can cause sharp conductance fluctuations—a kind of Fano resonance.^{8,9} For a quantum-dot system whose classical dynamics is either regular or contains a significant regular component, there are stable periodic orbits in the classical limit. If the dot geometry is closed, highly localized states can form around the classically stable periodic orbits. When electronic waveguides (leads) are attached to the quantum dot so that it is open, some periodic orbits can still survive, leading to resonant

states, or quantum pointer states. Since the corresponding classical orbits are stable, the resonant states can have long lifetime, so their coupling to the leads is weak. As a result, narrow resonances can form around the energy values that are effectively the eigenenergies for the stable periodic orbits in the corresponding closed system. When the dot geometry is modified so that the underlying classical dynamics becomes more and more chaotic, many of the periodic orbits become unstable. Although scars can still be formed around classically unstable periodic orbits in a closed chaotic system,¹⁰ the corresponding resonant states in the open system generally will have much shorter lifetimes. This means that these resonant states do couple to the leads more strongly, broadening the narrow resonances in the conductance-fluctuation pattern. Here, chaos is transient because the system is open. According to the theory of transient chaos,¹¹ the dynamical invariant sets responsible for transient chaos are non-attracting chaotic sets in the phase space. If the properties of transient chaos can be adjusted in the experiments by tuning some parameters, the quantum conductance fluctuation-patterns can then be harnessed in a desirable manner. If, in the future, nano-devices can be designed with voltage-control geometry, it may be possible to harness quantum system similar to controlling chaos. For example, one can change the effective geometry of the dot structure in a continuous manner so as to make the escape rate, a basic quantity characterizing transient chaos, to increase, and this could lead to significantly smoother quantum-conductance fluctuations.

There are two recent studies in the area of exploiting chaos for harnessing quantum behaviors: (1) the work of Pecora *et al.* in which fully developed Hamiltonian chaos was utilized to suppress the spread in the tunneling rate for any small energy interval (typically seen in classically integrable systems), or to regularize quantum tunneling dynamics,³ and (2) our recent brief note that transient chaos can be exploited to modulate conductance-fluctuation patterns in quantum dots.⁴ Here, we will provide a detailed analysis of the transient-chaos based quantum modulation paradigm. In particular, beyond the brief results in Ref. 4, extensive computational results will be presented to demonstrate the effectiveness of the paradigm and a comprehensive theory based on the generalized, non-Hermitian device Hamiltonian and the properties of its eigenstates will be developed to provide a solid foundation for the quantum-modulation strategy.

It is pertinent to discuss the issue of whether fully chaotic scattering dynamics is generic. When transient chaos coexists with stable periodic orbits, the corresponding dynamics is non-hyperbolic. Fully chaotic transient dynamics is hyperbolic in the sense that all periodic orbits are unstable. In a typical Hamiltonian system, when a parameter changes, nonhyperbolic dynamics can arise, followed by a transition to hyperbolic dynamics. However, both nonhyperbolic and hyperbolic dynamics can occur in *finite* parameter intervals. This was demonstrated in 1992 in a paradigmatic model of transition to chaotic scattering by Ding *et al.*¹² Regarding hyperbolic dynamics, there can even be direct transition from regular dynamics via the route of “abrupt bifurcation.”¹³ In any case, the typical feature is that hyperbolic dynamics exists in finite

parameter regime, indicating that hyperbolic transient chaos (or chaotic scattering) is generic. In our quantum-dot system, the basic geometry is that of an open Sinai billiard, which exhibits hyperbolic dynamics insofar as the radius of the central circle is non-zero. Transient chaos is in fact hyperbolic for all non-zero radius, and is thus generic. We note that even in dissipative dynamical systems, both nonhyperbolic and hyperbolic transient chaos can have finite measures in the parameter space.¹⁴

In Sec. II, we present the basic idea of chaos-based harnessing of quantum transport, propose an experimentally feasible scheme, and describe a layer-based non-equilibrium Green's function (NEGF) method that we optimize to compute the conductance through any quantum dot. Detailed simulation results are then presented in Sec. III using both traditional semiconductor 2DEG and graphene¹⁵ systems to demonstrate that transient chaos can effectively eliminate resonances associated with quantum transmission and make the conductance-fluctuation pattern markedly smoother. In Sec. IV, we provide a semiclassical argument based on existing works on quantum chaotic scattering to explain, qualitatively, why classical chaos can smooth out the quantum conductance fluctuations. Quantitatively, we develop a theory based on the concept of self-energies and the complex eigenvalue spectrum of the underlying generalized non-Hermitian Hamiltonian and obtain an explicit formula to predict the form of the narrow resonance. The analysis enables us to develop a self-consistent theoretical argument to fully explain our chaos-based harnessing scheme. A conclusion is presented in Sec. V.

II. PROPOSED EXPERIMENTAL SCHEME AND COMPUTATIONAL METHOD

Quantum-dot systems are a paradigm for investigating many kinds of quantum transport phenomena through nanostructures. Such a system typically consists of a finite device region of certain geometrical shape, such as a square, a circle, or a stadium, and a number of leads connected with the device region. To realize quantum harnessing by using chaos, we conceive generating a region about the center of the device or structure with high potential so that it is impenetrable to classical particles. For example, consider a rectangular quantum dot, a prototypical model in semiconductor 2DEG systems. When the dot is closed, the corresponding classical dynamics is integrable so that extremely narrow resonances can arise in the quantum transport dynamics of the open-dot system. Now imagine applying a gate voltage to generate a circular, classically forbidden region about the center of the dot, as shown schematically in Fig. 1. In general, the potential profile will be smooth in space. However, qualitatively, the scattering behavior is similar to that from an infinite potential well. Thus, in our simulation, we shall adopt the infinite potential-well assumption for the central region, which defines a “forbidden” region. Varying the voltage V_0 can change the effective radius R of the forbidden region. Classically, the closed system is thus a Sinai billiard,¹⁶ which is fully chaotic, insofar as the radius of the central potential region R is not zero. When leads are

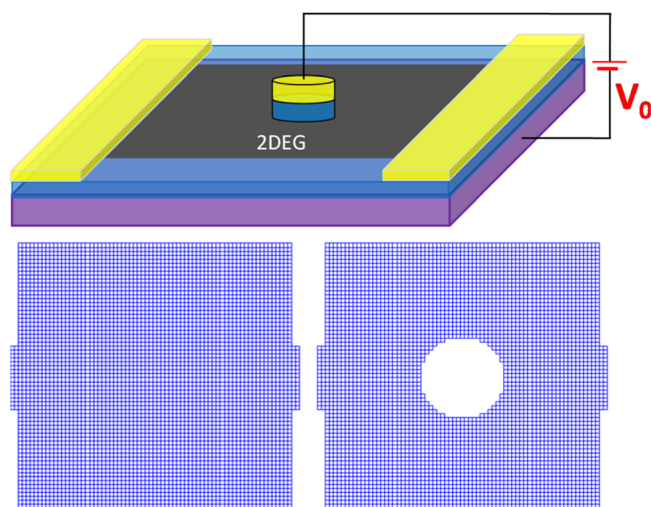


FIG. 1. Schematic illustration of a possible experimental scheme to harness transport through a semiconductor 2DEG quantum-dot system, where 2DEG is formed at the GaAs/Al_{0.3}Ga_{0.7}As hetero-interface. The heterostructure sits on a n⁺Si substrate (purple), covered by 300 nm SiO₂ (blue) and contacted by Au/Cr (yellow). By applying a suitable gate voltage to generate a *circular forbidden region* (for classical orbits) at the center of the device, the resulting closed system is a Sinai billiard. Open quantum-dot system can be formed by attaching leads to the billiard system. In this paper we place the leads in the middle of the dot, as shown in the second row. Similar idea can be applied to graphene systems.

connected to the device region so as to open the system, chaos becomes transient. The dynamical characteristics of the underlying chaotic invariant set can be adjusted in a continuous manner by increasing the radius R .¹⁷ Quantum mechanically we thus expect to observe increasingly smooth variations in the conductance with, e.g., the Fermi energy, which we will demonstrate using both semiconductor 2DEG and graphene systems.

We use the standard tight-binding framework to calculate the conductance/transmission and the local density of states (LDS). The tight-binding Hamiltonian is

$$\hat{H} = -t \sum |i\rangle\langle j| + \sum_i U(x_i, y_i) |i\rangle\langle i|,$$

where the first summation is over all pairs of nearest-neighbor atoms, and the second term describes the depletion potential. At low temperatures, the conductance G of a quantum dot is proportional to the quantum transmission T , as given by the Landauer formula^{5,18}

$$G(E) = (2e^2/h)T(E), \quad (1)$$

where E denotes the Fermi energy. Transmission is usually calculated by the NEGF method. For a quantum dot system consisting of a device region and two semi-infinite leads (left lead and right lead), the transmission can be calculated through the self-energies.⁵ In particular, let H_D (“D” denotes device) be the finite Hamiltonian matrix describing the device in the tight-binding framework. The Green’s function of the device is given by

$$G_D = (EI - H_D - \Sigma_L - \Sigma_R)^{-1}, \quad (2)$$

where I is the identity matrix of the same size of H_D , Σ_L , and Σ_R are the self-energies associated with the left and right leads, respectively. Let $U_{L,R}$ be the coupling matrix between the left (right) lead with the device, the self-energies $\Sigma_{L,R}$ for the left and right leads can be calculated self-consistently by the following Dyson's equations:¹⁹

$$\Sigma_{L,R} = U_{L,R}^\dagger (E - H_D - \Sigma_{L,R})^{-1} U_{L,R}. \quad (3)$$

The transmission is then given by

$$T(E) = \text{Tr}(\Gamma_L G_D \Gamma_R G_D^\dagger), \quad (4)$$

where $\Gamma_{L,R} \equiv i(\Sigma_{L,R} - \Sigma_{L,R}^\dagger)$. The LDS for the device is

$$\rho_j = -\frac{1}{\pi} \text{Im}[\text{diag}(G_D)]. \quad (5)$$

Although the above procedure is standard, for quantum dots of large sizes (e.g., size of 100 nm), the size of the device Hamiltonian matrix H_D will be large, making the computation extremely demanding even using computers with large memory capacity. We are thus led to develop a layer-by-layer type of recursive Green's function (RGF) method to calculate the transmission and the local density of states. The basic idea is to divide a given (large) device into smaller units or layers. The specific way to choose the division can be highly flexible, depending on the geometrical shape of the device region. A well-designed, physically meaningful division scheme can help accelerate the computation. Say, we divide the device into N layers. The left and right leads can be conveniently labeled as layer 0 and layer $N+1$, respectively. In our RGF method, each layer j ($j=1, \dots, N$) is considered as a separated device and its nearest neighboring layers $j-1$ and $j+1$ are regarded as the local left and right "leads" connecting to the device j , respectively. The Green's function G_j of the layer j is determined by the Fermi energy and the self-energies from its "leads." Carrying out the calculation of the Green's function layer-by-layer, we can assemble the Green's function for the original (large) device.

The merits of our RGF method lie in its time and memory efficiency for large device simulations, its high accuracy, and the flexibility to treat device of arbitrary geometrical shape. The method is not limited to the calculation of transport properties for open systems. In fact, by imposing the zero-contact condition at the boundaries of the leads, our RGF method can be adopted to closed system calculations. Extensive tests indicate that our RGF method outperforms the conventional NEGF method in the computational efficiency by up to three orders of magnitude.

III. NUMERICAL RESULTS

To demonstrate the working of our scheme, we compute and compare the conductance-fluctuation patterns of four different quantum-dot geometries: rectangular dot, rectangular dot with a rectangular forbidden region, which is mainly for comparison, and two Sinai dots. The classical dynamics are integrable for the first two cases and fully chaotic for the latter two cases. For all the geometries, we assume that the dot

systems are of either semiconductor 2DEG or graphene, and we calculate the quantum transmission as a function of the Fermi energy, as shown in Fig. 2(a) for semiconductor 2DEG quantum dots and in Fig. 2(b) for graphene dots. Qualitatively, we observe the appearance of sharp resonances in the transmission curves for the integrable dots, while the curves appear smoother in the chaotic cases. To quantify and compare the transmission fluctuations, we calculate the number N of sharp resonances associated with each curve, which are defined as those whose energy width is smaller than some threshold value ε . We use $\varepsilon = 5 \times 10^{-3}$ meV in this paper. Figure 2(c) shows the values of N for the four semiconductor 2DEG quantum dots in Fig. 2(a). By comparing the top two rectangular symbols, that denote the two integrable quantum dots, we observe a small difference in the sense that the numbers of sharp resonances are approximately the same. However, for the chaotic Sinai quantum dots, denoted by the circles, there are markedly fewer sharp resonances. These results illustrate that, generating a forbidden region at the center of the rectangular dot is not necessarily effective in removing the narrow resonances in the quantum transmission curve (e.g., comparing the two integrable cases: the top red rectangular symbols). It is *chaos* which is effective in eliminating the resonances (e.g., comparing the middle rectangular and circle symbols). Similar behaviors have been observed for the graphene quantum dots.

In our simulation, we have checked the effect of varying lead sizes. When keeping the quantum dot unchanged and increasing the width of the leads, the conductance fluctuations will be smoother, i.e., with fewer sharp resonances. While this appears to have a similar effect to that due to chaos, the physical mechanism is quite different. In this case,

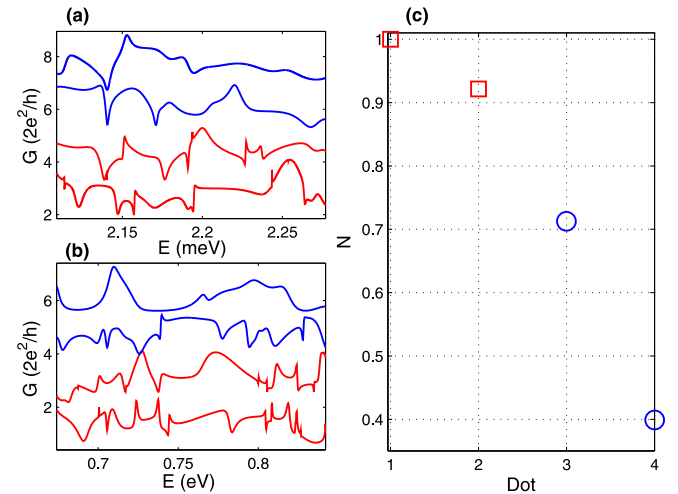


FIG. 2. (a) Conductance versus Fermi energy for four semiconductor 2DEG quantum-dot systems (bottom to top): rectangular dot, rectangular dot with a rectangular forbidden region of area $0.25 \mu\text{m} \times 0.25 \mu\text{m}$, and Sinai dots of radii $R = 0.14 \mu\text{m}$ and $R = 0.28 \mu\text{m}$. The area of the original rectangular dot is $1 \mu\text{m} \times 1 \mu\text{m}$ and the lead width is $0.22 \mu\text{m}$. (b) Conductance fluctuation patterns for graphene quantum dots of the same geometry as in (a).²⁰ The curves in (a) and (b) have been shifted vertically by some arbitrary values to facilitate visualization. (c) Normalized number of *sharp resonances*, which is defined (see text) to quantify the degree of transmission fluctuations, corresponding to the four cases in (a), i.e., the top two rectangular symbols represent two rectangular quantum dots while the bottom two circles correspond to two Sinai quantum dots.

the effect is due to the stronger coupling between the lead and the dot when the leads become larger, as we will discuss in the theory part regarding the self-energy σ_R . However, for any given lead size, when varying the dots, we can observe the similar effect that Sinai billiards with larger forbidden region exhibit fewer sharp resonances.

Figure 3 shows, for semiconductor 2DEG quantum dots with a circular central forbidden region, N versus the radius R , which is normalized by the number of sharp resonances in the $R=0$ case. We check systematically the effect of the radius on conductance fluctuations, i.e., the number of sharp resonances for a certain energy interval, and observe an approximately linear relation between N and R . We see that, as the radius of the forbidden region is increased, there is continuous improvement in the smoothness of the fluctuation patterns since the number of sharp resonances decreases continuously and drastically. In the corresponding classical chaotic Sinai billiard system, we find that the escape rate of the underlying non-attracting chaotic set increases with the radius, as shown in Fig. 4, a contour plot of the escape rate in the parameter plane of W and R , where W is the width of the leads. For a fixed value of W , we see that the escape rate increases with R .¹⁷ There is thus strong correspondence between the quantum and classical behaviors in Figs. 3 and 4, respectively, through the escape rate, the most fundamental characterizing quantity in the theory of transient chaos.¹¹ These results show that our chaos-based method provides one possible solution to systematically harness or regularize quantum transport, which could potentially be implemented and observed in experiments.²¹

IV. THEORY

Qualitatively, the occurrence of shape resonances in the conductance versus the Fermi energy can be understood by the emergence of quantum pointer states.⁷ A closed integrable system possesses a large number of stable periodic orbits in the classical limit. As resulting from quantum

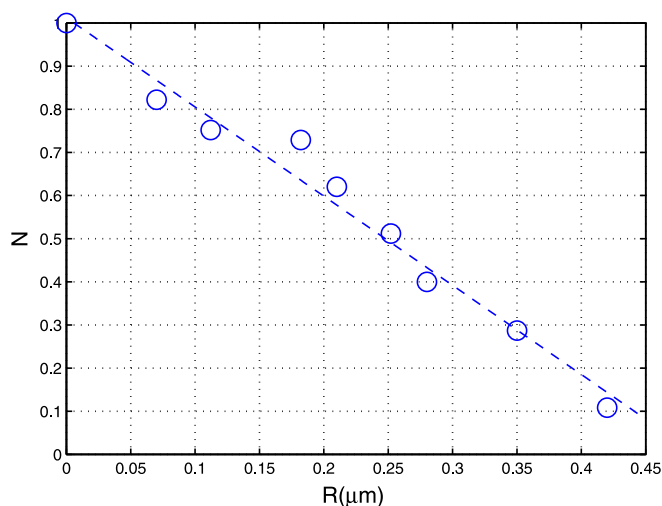


FIG. 3. Normalized number of sharp resonances versus radius of the central circular forbidden region [Fig. 1]. The area for original rectangular quantum dot is $1 \mu\text{m} \times 1 \mu\text{m}$.

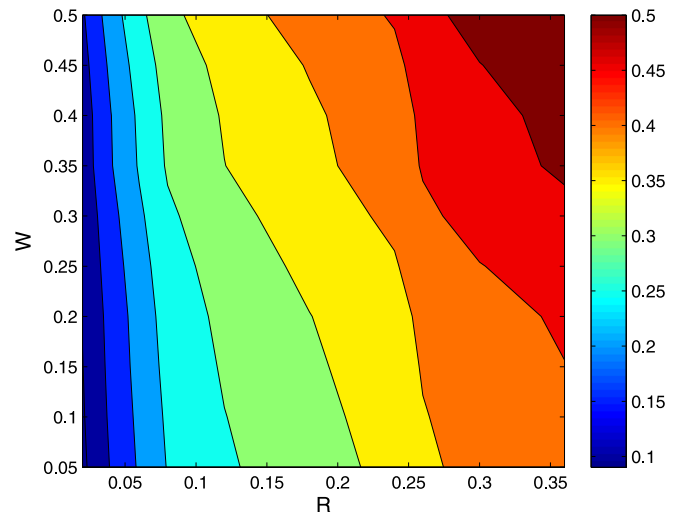


FIG. 4. Contour plot of escape rate in the parameter plane of W and R . For each parameter combination, 10^6 random particles, each of unit velocity, are used to calculate the escape rate. For each particle, its path length in the scattering region (the Sinai billiard region) is calculated. The distribution of the path length is observed to decay exponentially, and the escape rate is the exponential rate.

interference, eigen-wavefunctions are expected to be highly non-uniform in the physical space in that they concentrate around the classically stable periodic orbits. When leads are connected to the system (device), so that it becomes open, some of the eigenstates are destroyed but many can survive. If the size of the opening is small compared with the size of the device, the coupling between it and the leads is weak. These surviving eigenstates are the pointer states.⁷ As the Fermi energy is changed, electrons encounter various pointer states. When a pointer state emerges, the electron wavefunction tends to be localized in the device, causing a sharp change in the conductance. Thus we expect the conductance versus energy curve to exhibit a large number of sharp resonances. However, when the classical dynamics in the closed system becomes fully chaotic, almost all periodic orbits are unstable.²² In this case, while quantum scars can still form around some of the unstable periodic orbits,¹⁰ they are less likely to “survive” when the system becomes open. As a result, it is more difficult for pointer states to form in an open chaotic system, leading to smoother conductance fluctuations.

Insights into why classical chaos can smooth out quantum conductance fluctuations can also be gained from semiclassical theory of quantum chaotic scattering.^{23,24} In particular, in the semiclassical regime, it was established by Blümel and Smilansky that the energy autocorrelation function of the quantum transmission fluctuation is proportional to the Fourier transform of the particle-decay law in the classical limit.²³ For fully developed chaotic transport through a quantum dot, the decay law is exponential with the rate κ . As a result, the quantum energy correlation function decays as a Lorentzian function with the width given by $\hbar\kappa$. In the theory of transient chaos,¹¹ κ is the escape rate associated with the underlying non-attracting chaotic set. As the radius of the central potential region is increased, κ also increases.¹⁷ As a result, the energy autocorrelation function decays more slowly,

signifying less fluctuations, i.e., less number of *sharp resonances* in the quantum transmission. This semiclassical argument suggests that the degree of quantum transmission fluctuations can be harnessed by classical chaos.

To understand quantitatively the mechanism of chaos-based harnessing of quantum transport, we now develop a physical theory by focusing on the transmission resonances and the coupling²⁵ between the eigenstates in the quantum dot and leads. Under the tight-binding paradigm, the scattering region can be regarded as a closed system of Hamiltonian matrix H_D and the effect of the leads can then be treated using the retarded self-energy matrices

$$\Sigma^R = \Sigma_L^R + \Sigma_R^R. \quad (6)$$

The matrix H_D is Hermitian with a set of real eigenenergies and eigenfunctions $\{E_{0\alpha}, \psi_{0\alpha}\}$, where $\{\psi_{0\alpha}|\alpha = 1, \dots, N\}$ form a complete and orthogonal basis set. However, $\Sigma^R(E_0)$ is in general not Hermitian and depends on the Fermi energy E_0 . The effective Hamiltonian matrix $H_D + \Sigma^R(E_0)$ thus has a set of complex eigenenergies with the eigenfunctions

$$[H_D + \Sigma^R(E_0)]\psi_\alpha = E_\alpha \psi_\alpha, \quad (7)$$

where

$$E_\alpha = E_{0\alpha} - \Delta_\alpha - i\gamma_\alpha, \quad (8)$$

Δ_α is a shift in the eigenenergy of the closed system induced by Σ^R , and γ_α characterizes the energy scale of the transmission resonance caused by ψ_α .^{5,26}

We can use the perturbation theory, similar to Eq. (8), to obtain a better understanding of the behavior of the key quantity γ_α . In particular, we can express the eigenfunctions of the open system as

$$\psi_\alpha = \psi_{0\alpha} - \delta_r \psi_{\alpha r} - i\delta_i \psi_{\alpha i}, \quad (9)$$

where $\delta_{r(i)}$ represents a small perturbation on the real (imaginary) part of ψ_α induced by the self energy Σ^R , and $\psi_{\alpha r}$ and $\psi_{\alpha i}$ can be represented by the eigenfunction basis set $\psi_{0\beta}$ of the Hamiltonian matrix H_D for the closed system, i.e.,

$$\begin{cases} \psi_{\alpha r} = \sum_{\beta} C_{\beta r} \psi_{0\beta}, \\ \psi_{\alpha i} = \sum_{\beta} C_{\beta i} \psi_{0\beta}, \end{cases} \quad (10)$$

where $C_{\beta(r,i)}$ are the expansion coefficients for state β .

Substituting Eqs. (8) and (9) back into Eq. (7), we have

$$\begin{aligned} (H_D + \Sigma^R)(\psi_{0\alpha} - \delta_r \psi_{\alpha r} - i\delta_i \psi_{\alpha i}) \\ = (E_{0\alpha} - \Delta_\alpha - i\gamma_\alpha)(\psi_{0\alpha} - \delta_r \psi_{\alpha r} - i\delta_i \psi_{\alpha i}). \end{aligned}$$

Keeping the first-order terms on both sides and taking into account the fact that, for the closed system, the relation $H_D \psi_{0\alpha} = E_{0\alpha} \psi_{0\alpha}$ holds, we get

$$\begin{aligned} H_D(\delta_r \psi_{\alpha r} - i\delta_i \psi_{\alpha i}) + \Sigma^R \psi_{0\alpha} \approx (\Delta_\alpha + i\gamma_\alpha) \psi_{0\alpha} \\ + E_{0\alpha}(\delta_r \psi_{\alpha r} + i\delta_i \psi_{\alpha i}). \end{aligned} \quad (11)$$

Substituting Eq. (10) into this equation, multiplying $\langle \psi_{0\alpha} | \cdot \rangle$ on both sides, and using $\langle \psi_{0\alpha} | \psi_{0\beta} \rangle = \delta_{\alpha\beta}$, we obtain

$$\Delta_\alpha + i\gamma_\alpha \approx -\langle \psi_{0\alpha} | \Sigma^R | \psi_{0\alpha} \rangle. \quad (12)$$

We thus have

$$E_\alpha = E_{0\alpha} - \Delta_\alpha - i\gamma_\alpha \approx E_{0\alpha} + \langle \psi_{0\alpha} | \Sigma^R | \psi_{0\alpha} \rangle. \quad (13)$$

The resonance width is given by

$$\gamma_\alpha \approx -\text{Im}(\langle \psi_{0\alpha} | \Sigma^R | \psi_{0\alpha} \rangle) = -\langle \psi_{0\alpha} | \text{Im}(\Sigma^R) | \psi_{0\alpha} \rangle, \quad (14)$$

which is determined by the imaginary part of the self-energy Σ^R and the corresponding eigen-wavefunction $\psi_{0\alpha}$ of the closed system. In general, Σ^R can be expressed as⁵

$$\Sigma^R = -t \sum_L \sum_{m \in L} \chi_{m,L} \exp(ik_m a) \chi_{m,L}^\dagger, \quad (15)$$

where L is the lead index and $\chi_{m,L}$ is the eigenfunction of mode m in lead L . The energy dependence is contained in $k_m(E)$. Since Σ^R only has nonzero elements at the boundary points of the device connecting with the leads, only the values of $\psi_{0\alpha}$ on the same set of discrete points, $\psi_{0\alpha,L}$, contribute to γ_α . Since $\{\chi_{m,L}\}$ form a complete and orthogonal basis, $\psi_{0\alpha,L}$ can be expanded as $\psi_{0\alpha,L} = \sum_m c_m \chi_{m,L}$. Substituting this back into Eq. (13) and noting that the system has left-right mirror symmetry, we obtain

$$E_\alpha \approx E_{0\alpha} - 2t \sum_m |c_m|^2 \exp(ik_m a). \quad (16)$$

To validate our first-order approximation analysis, we take one small rectangular QD as an example, as shown in Fig. 5, where the dot area is $0.2 \mu\text{m} \times 0.2 \mu\text{m}$ and the number of discrete points used in the simulation is 218. Since Σ^R depends on E_0 , Δ_α and γ_α are also functions of E_0 . Thus our

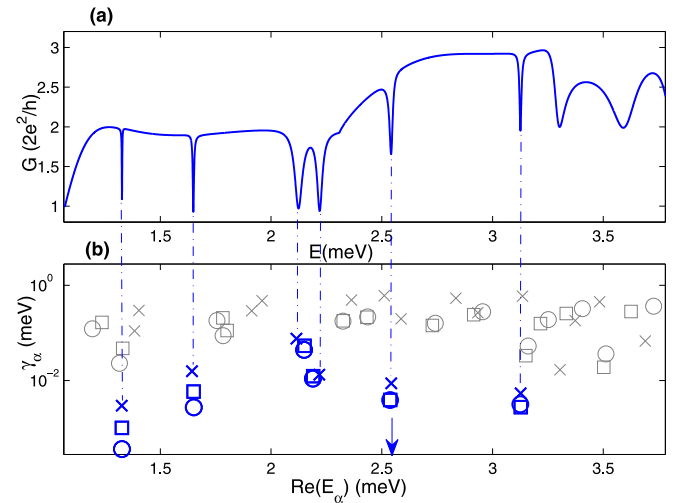


FIG. 5. (a) Conductance versus energy for one small quantum dot of area $0.2 \mu\text{m} \times 0.2 \mu\text{m}$, where the number of discrete points used in the simulation is 218; (b) the corresponding imaginary parts versus real parts of eigenenergy E_α of $H_D + \Sigma^R(E_0)$ (cross), calculated from Eq. (13) (square) and Eq. (16) (circle). The Fermi energy is $E_0 = 2.5293 \text{ meV}$, as indicated by the arrow.

theory is valid only for eigenstates whose values of $\text{Re}(E_\alpha)$ are close to E_0 .⁵ In Fig. 5(b), we use $E_0 = 2.5293$ meV. We observe a good correspondence of the positions of the transmission resonances and their width to the real and imaginary parts of the eigenenergies of $H_D + \Sigma^R(E_0)$ (crosses), respectively. The eigenstates whose values of γ_α are approximately 10^{-1} meV contribute to the smooth, background conductance variations. However, eigenstates whose γ_α values are in the range 10^{-3} meV to 10^{-2} meV correspond to localized states, for example, the five states indicated by the dashed-dotted lines. Our results based on Eq. (13) (square) and Eq. (16) (circle) agree with the simulation results (crosses) reasonably well, especially for $\text{Re}(E_\alpha)$ near E_0 .

Our analysis of the complex eigenvalues of the generalized Hamiltonian leads to two observations. First, since γ_α characterizes the energy scale of the conductance resonance, the degree of the conductance fluctuations can be inferred from the distribution of γ_α values. In particular, smaller γ_α values indicate more severe conductance fluctuations. Second, the values of γ_α mainly depend on the projection of the eigenfunction coupled to the lead onto the eigenfunction of the lead itself, i.e., c_m in Eq. (16). As a result, the morphology of the eigenfunction, especially the amplitude at the lead region, plays an important role in determining γ_α and the conductance fluctuations. These observations can be used to elucidate the physical origin of chaos-based harnessing of conductance fluctuations, as follows.

First, Fig. 6 shows the distribution of γ_α in a proper energy range, where Σ^R is evaluated at $E_0 = 2.7862$ meV. We see that in Fig. 6(a), the values of γ_α spread out far below 5×10^{-4} meV, even to 10^{-6} meV. The corresponding eigenstates are thus the localized states in the rectangular quantum dot, leading to sharp resonances on the energy scale of 10^{-4} meV. However, for the chaotic Sinai quantum dots,

most values of γ_α are concentrated above 5×10^{-4} meV, as shown in Figs. 6(c) and 6(d). This indicates the disappearance of sharp conductance resonances. Note that the integrable quantum dot with a central rectangular forbidden region [Fig. 6(b)] has approximately the same number of eigenstates as the chaotic Sinai quantum dot with $R = 0.14 \mu\text{m}$, but the distributions of γ_α values are different for the two cases in that there are significantly more points below the reference line in the integrable dot than in the chaotic dot, indicating more severe conductance fluctuations in the integrable case. Consequently, the number of sharp resonances will be smaller for the chaotic quantum dots. As R is increased, the classical escape rate becomes larger; there is a progressive disappearance of eigenvalues with extremely small imaginary parts. The number of resonances of extremely narrow width decreases, leading to smoother fluctuation patterns.

Second, since Σ^R is calculated from the leads, it only depends on the width of the leads and the Fermi energy. It is thus the same for all the quantum dots we have considered above for a fixed energy E_0 . The difference in the values of γ_α is solely determined by the quantity c_m , which is the projection of the eigenfunction coupled to the lead, $\psi_{0\alpha,L}$, onto the eigenfunction of the lead itself, $\chi_{m,L}$. For the integrable quantum dots, there are localized states corresponding to the stable orbits. As a result, these states couple to the leads only weakly, leading to smaller values of c_m . For the chaotic quantum dots with relatively large escape rates, unstable periodic orbits dominate, so the resonant states are not as pronounced as for the integrable dots, leading to a larger component on the leads and hence larger values of c_m . These considerations can be demonstrated directly from the LDS patterns, as shown in Fig. 7. For the integrable QDs without the central forbidden region [Fig. 7(a)], the LDS patterns associated with the resonant states are well localized. The

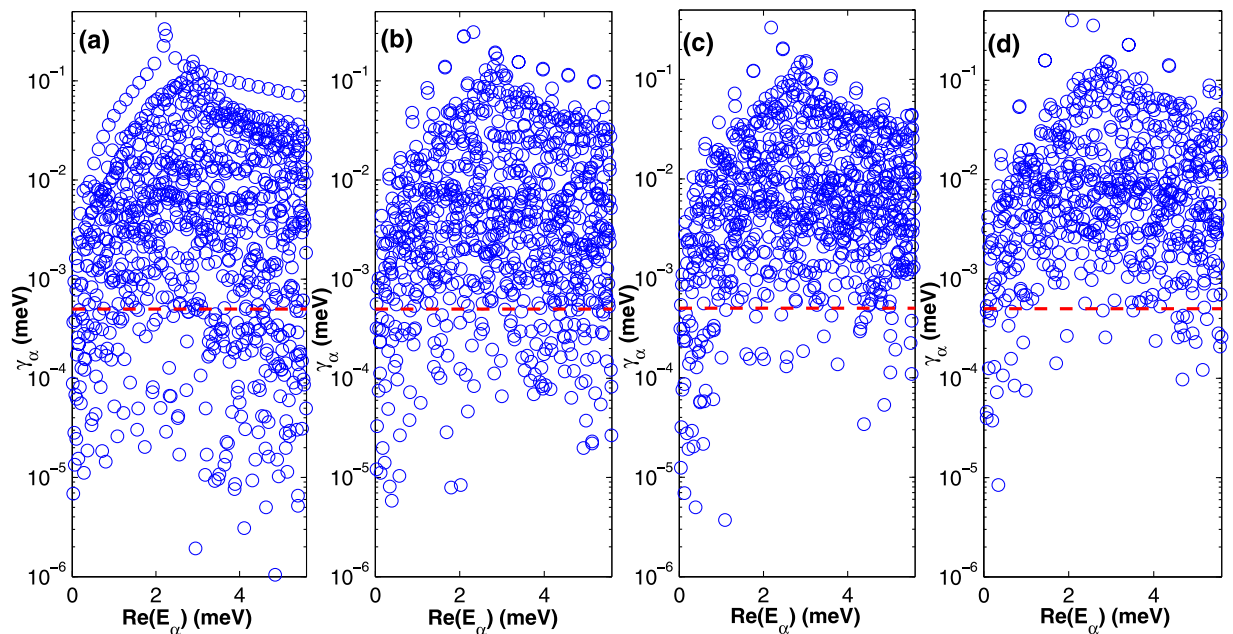


FIG. 6. Imaginary and real parts of the eigenenergies E_α for (a) rectangular quantum dot, (b) rectangular dot with a rectangular forbidden region at the center, (c) Sinai quantum dot with $R = 0.14 \mu\text{m}$, and (d) Sinai dot with $R = 0.28 \mu\text{m}$, where $E_0 = 2.7862$ meV for all cases. Each eigenenergy is represented by one blue circle. The red dashed lines indicate $\gamma_\alpha = 5 \times 10^{-4}$ meV and they are just for eye guidance.

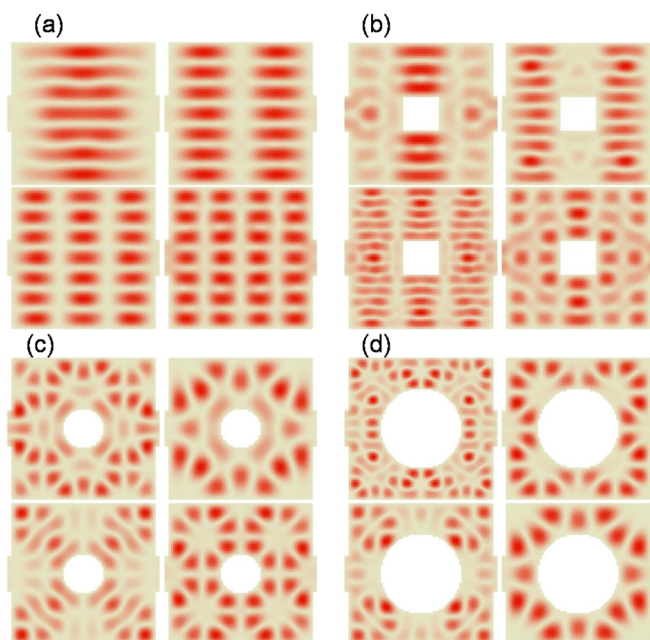


FIG. 7. Typical quantum pointer states for (a) rectangular quantum dot, (b) rectangular quantum dot with a rectangular forbidden region, (c) and (d) Sinai quantum dots of radii $R = 0.14 \mu\text{m}$ and $R = 0.28 \mu\text{m}$, respectively. Darker regions indicate higher values of LDS. The color scale has been normalized for each panel for better visualization. The mean value of LDS in the leads are 0.0154, 0.0351, 0.0491, 0.0669 for panels (a)-(d), respectively. We observe the presence of pronounced pointer states in the two integrable cases.

patterns are mainly those corresponding to the classical “bouncing-ball” orbits. One can see that the values of the LDS on the leads are indeed quite small. When a rectangular forbidden region is present in the central region, the system is still classically integrable, which has no significant effect on the LDS patterns, as shown in Fig. 7(b). For the chaotic Sinai dots, the LDS patterns are strongly affected by the central circular forbidden region in that they appear much less localized and relatively more uniform than those in the integrable dots, as can be seen from Figs. 7(c) and 7(d). This typically leads to much larger LDS values on the leads, resulting in larger values of the wavefunction at the boundaries of the quantum dot and, hence, strong coupling with the leads.

V. CONCLUSIONS

We have proposed and demonstrated that classical transient chaos can be used to effectively harness quantum transport fluctuations both in the non-relativistic quantum regime, where the dot is a semiconductor 2DEG system, and in the relativistic quantum regime, where the whole system is made up of graphene. The key underlying physics is that chaos in the classical limit has a profound effect on the emergence of resonant states in the corresponding quantum transport system. As the escape rate associated with transient chaos is increased, pointer states, which are ubiquitous in open integrable systems, become increasingly difficult to survive, and they tend to be less localized with shorter lifetimes. This effect significantly enhances the coupling between the eigenstates in the device and in the leads.

We have developed a physical theory to unveil the relations between the characteristic energy scale of the conductance resonance and the eigenstates in the corresponding closed system, showing that integrable quantum dots possess highly localized states, leading to very weak coupling to the leads and resulting in extremely narrow conductance resonances. When the classical dynamics becomes fully chaotic, the opposite effects arise, namely, less localized (more dispersive) states, stronger coupling to the leads, and broadened conductance resonance. These theoretical insights suggest that, by applying a gate voltage generating the inaccessible regions so that the originally integrable system changes to being chaotic, quantum conductance fluctuations can be made smoother. Continuous modulation or harnessing of the conductance-fluctuation patterns is possible by increasing the gate voltage systematically. As a result, conductance fluctuations, a key characteristic associated with quantum transport, can be regularized via transient chaotic dynamics in the classical limit. Our chaos-based quantum harnessing scheme is conceptually appealing and experimentally feasible, and further interest and effort are warranted to explore this concept for significant applications in nanoscience and nanotechnology where quantum transport is fundamental.

Finally, we remark that, in the OGY paradigm of controlling chaos,¹ small parameter changes are used to stabilize the system about some desirable unstable periodic orbit. An appealing feature is to take advantage of chaos to control the system toward some desirable performing state. This is in fact the spirit of our work, i.e., to use chaos to do “good.” In particular, we have proposed an experimentally feasible method to regularize quantum transport, i.e., to broaden the transmission resonances and make the transmission curve smooth. The common feature with the OGY method is that in both cases, chaos is exploited for a purpose. For example, it is possible to apply small perturbations to stabilize a chaotic system about any desirable state. In our case, chaotic scattering is utilized to reduce the sharpness in conductance fluctuations, although the “perturbation” occurs in the system structure and is not necessarily small.

ACKNOWLEDGMENTS

We thank P.-P. Li for assisting in generating Fig. 4. This work was supported by AFOSR under Grant No. FA9550-12-1-0095 and by ONR under Grant No. N00014-08-1-0627. L.H. was also supported by NSFC under Grant No. 11005053.

¹E. Ott, C. Grebogi, and J. A. Yorke, *Phys. Rev. Lett.* **64**, 1196 (1990).

²S. Boccaletti, C. Grebogi, Y.-C. Lai, H. Mancini, and D. Maza, *Phys. Rep.* **329**, 103 (2000).

³L. M. Pecora, H. Lee, D.-H. Wu, T. Antonsen, M.-J. Lee, and E. Ott, *Phys. Rev. E* **83**, 065201 (2011).

⁴R. Yang, L. Huang, Y.-C. Lai and L. M. Pecora, *Appl. Phys. Lett.* **100**, 093105 (2012).

⁵S. Datta, *Electronic Transport in Mesoscopic Systems* (Cambridge University Press, Cambridge, UK, 1995).

⁶See, for example, R. A. Jalabert, H. U. Baranger, and A. D. Stone, *Phys. Rev. Lett.* **65**, 2442 (1990); R. Ketzmerick, *Phys. Rev. B* **54**, 10841 (1996); R. P. Taylor, R. Newbury, A. S. Sachrajda, Y. Feng, P. T.

- Coleridge, C. Dettmann, Ningjia Zhu, Hong Guo, A. Delage, P. J. Kelly, and Z. Wasilewski, *Phys. Rev. Lett.* **78**, 1952 (1997); A. S. Sachrajda, R. Ketzmerick, C. Gould, Y. Feng, P. J. Kelly, A. Delage, and Z. Wasilewski, *ibid.* **80**, 1948 (1998); B. Huckestein, R. Ketzmerick, and C. H. Lewenkopf, *ibid.* **84**, 5504 (2000); G. Casati, I. Guarneri, and G. Maspero, *ibid.* **84**, 63 (2000); R. Crook, C. G. Smith, A. C. Graham, I. Farrer, H. E. Beere, and D. A. Ritchie, *ibid.* **91**, 246803 (2003).
- ⁷W. H. Zurek, *Rev. Mod. Phys.* **75**, 715 (2003); R. Akis, J. P. Bird, and D. K. Ferry, *Appl. Phys. Lett.* **81**, 129 (2002); D. K. Ferry, R. Akis, and J. P. Bird, *Phys. Rev. Lett.* **93**, 026803 (2004).
- ⁸U. Fano, *Phys. Rev.* **124**, 1866 (1961).
- ⁹H. Ishio, *Phys. Rev. E* **62**, R3035 (2000).
- ¹⁰Given a closed Hamiltonian system that exhibits fully developed chaos in the classical limit, one might expect the quantum wavefunctions associated with various eigenstates to be more or less uniform in the physical space. However, in the seminal work of McDonald and Kaufman [*Phys. Rev. Lett.* **42**, 1189 (1979) and *Phys. Rev. A* **37**, 3067 (1988)], it was observed that quantum eigen-wavefunctions can be highly non-uniform in the chaotic stadium billiard. A systematic study was subsequently carried out by Heller [*Phys. Rev. Lett.* **53**, 1515 (1984)], who established the striking tendency for wavefunctions to concentrate about classical unstable periodic orbits, which he named *quantum scars*. Semiclassical theory was then developed by Bogomolny [*Physica D* **31**, 169 (1988)] and Berry [*Proc. R. Soc. London, Ser. A* **423**, 219 (1989)], providing a general understanding of the physical mechanism of quantum scars. The phenomenon of quantum scarring was deemed counterintuitive and surprising but only for chaotic systems, as the phase space of an integrable system is not ergodic so that the quantum wavefunctions are generally not expected to be uniform. Relativistic quantum scars in chaotic graphene and Dirac fermion systems have also been reported [L. Huang, Y.-C. Lai, D. K. Ferry, S. M. Goodnick, and R. Akis, *Phys. Rev. Lett.* **103**, 054101 (2009); H.-Y. Xu, L. Huang, Y.-C. Lai, and C. Grebogi, *Phys. Rev. Lett.* **110**, 064102 (2013)].
- ¹¹Y.-C. Lai and T. Tél, *Transient Chaos* (Springer, New York, 2011).
- ¹²M. Ding, C. Grebogi, E. Ott, and J. A. Yorke, *Phys. Rev. A* **42**, 7025 (1990).
- ¹³S. Bleher, C. Grebogi, and E. Ott, *Physica D* **45**, 87 (1990).
- ¹⁴Y.-C. Lai, C. Grebogi, J. A. Yorke, and I. Kan, *Nonlinearity* **6**, 779 (1993).
- ¹⁵K. S. Novoselov, A. K. Geim, S. V. Morozov, D. Jiang, Y. Zhang, S. V. Dubonos, I. V. Grigorieva, A. A. Firsov, *Science* **306**, 666 (2004); C. Berger, Z. Song, T. Li, X. Li, A. Y. Ogbazghi, R. Feng, Z. Dai, A. N. Marchenkov, E. H. Conrad, P. N. First, W. A. de Heer, *J. Phys. Chem. B* **108**, 19912 (2004); C. W. J. Beenakker, *Rev. Mod. Phys.* **80**, 1337 (2008); A. H. Castro Neto, F. Guinea, N. M. R. Peres, K. S. Novoselov, and A. K. Geim, *Rev. Mod. Phys.* **81**, 109 (2009).
- ¹⁶Y. Sinai, *Russ. Math. Surveys* **25**, 137 (1970).
- ¹⁷Qualitatively, the escape rate is the inverse of the average lifetime of transient chaos. Increasing the radius of the circular forbidden region makes more difficult for particles to stay in the scattering region, leading to a decrease in the lifetime. As a result, the escape rate increases.
- ¹⁸R. Landauer, *Philos. Mag.* **21**, 863 (1970).
- ¹⁹T. C. Li, S. Lu, *Phys. Rev. B* **77**, 085408 (2008); L. Huang, Y.-C. Lai, D. K. Ferry, R. Akis, and S. M. Goodnick, *J. Phys.: Condens. Matter* **21**, 344203 (2009).
- ²⁰For graphene quantum dots, we use relatively small size as compared with the 2DEG (the size of the original rectangular graphene sheet is 15 nm × 15 nm and the number of atoms are around 8000). Also, for the Sinai quantum dots denoted by the circular forbidden region and green curves in Fig. 2(b), the radii are $R = 2.5$ nm and $R = 5$ nm, respectively. Thus, the Fermi energies are larger than those for 2DEG. However, for both Figs. 2(a) and 2(b), the energy ranges normalized by the hopping energy t of the nearest neighbors are the same, i.e., $\Delta E/t = 0.06$.
- ²¹While at the present there is no direct experimental support for our proposed scheme of chaos-based modulation of quantum transport, previous experimental and computational works on 2DEG, Sinai-type of quantum billiard provided *indirect* justification for our scheme, like [J. P. Bird, *J. Phys.: Condens. Matter* **11**, 413 (1999); R. Akis and D. K. Ferry, *Phys. Rev. B* **59**, 11 (1999).]
- ²²Even for a chaotic billiard, there can be marginally stable periodic orbits, such as the vertically bouncing orbits in the rectangular region of a chaotic stadium billiard, and vertically or horizontally bouncing orbits in the Sinai billiard. These orbits can lead to sharp resonances in the quantum conductance.
- ²³R. Blümel and U. Smilansky, *Phys. Rev. Lett.* **60**, 477 (1988); *Physica D* **36**, 111 (1989).
- ²⁴Y.-C. Lai, R. Blümel, E. Ott, and C. Grebogi, *Phys. Rev. Lett.* **68**, 3491 (1992).
- ²⁵K. Pichugin, H. Schanz, and P. Seba, *Phys. Rev. E* **64**, 056227 (2001).
- ²⁶R. Yang, L. Huang, Y.-C. Lai, and C. Grebogi, *Europhys. Lett.* **94**, 40004 (2011).